The Suppression of Commutation Torque Ripple in Brushless DC Motors Based on Segmental Duty Cycle Distribution

Zhiduan Cai
Huzhou College
Jiahao Shen
Huzhou University
Lihao Xu
xulihao@zjhzu.edu.cn
Huzhou College
Yuling Wang
Huzhou College

Article

Keywords: Brushless DC motor, Braking, Commutation torque ripple, Overlapping commutation, PWM-OFF-PWM

Posted Date: January 9th, 2025

DOI: https://doi.org/10.21203/rs.3.rs-5741730/v1

Additional Declarations: No competing interests reported.

The Suppression of Commutation Torque Ripple in Brushless DC Motors Based on Segmental Duty Cycle Distribution

Zhiduan Cai[1], Jiahao Shen[2], Lihao Xu[1,*], Yuling Wang[1]

*email:xulihao@zjhzu.edu.cn

1. School of Intelligent Manufacturing, Huzhou College, Huzhou, Zhejiang, China.
2. School of Engineering, Huzhou University, Huzhou, Zhejiang, China.

Abstract

During the commutation process of brushless direct current (BLDC) motors, significant commutation torque pulsations occur, which degrade the operational performance and efficiency of the motor. Conventional overlapping commutation methods can effectively suppress commutation torque pulsations; however, they are susceptible to issues related to control fail areas. In response to this challenge, the paper presents an improved segmented duty cycle allocation method for overlapping commutation, which effectively suppresses commutation torque pulsations during the braking process across a wide range of speeds. This commutation method employs a PWM-OFF-PWM modulation technique, which allocates differing duty cycles based on the high and low speed segments during the commutation period. Each speed segment independently undergoes pulse width modulation for either the conducting phase or the non-conducting phase, ensuring that the rate of current rise in the conducting phase is matched by the rate of current decline in the non-conducting phase during commutation. This synchronization allows for a smooth transition of non-commutating phase currents during the commutation period, thereby reducing commutation torque pulsations. Compared to conventional overlapping commutation methods, the proposed technique not only eliminates the control fail area issue induced by delayed control strategies, but also decreases the switching frequency of the power switch transistors, thus reducing switching losses. The feasibility, effectiveness and superiority of the proposed method are demonstrated in experiments.

Keywords Brushless DC motor; Braking; Commutation torque ripple; Overlapping commutation; PWM-OFF-PWM

1 Introduction

The brushless direct current motor (BLDCM) is an electrical equipment widely used in both industry and daily life. The optimization of the control strategy is crucial for improving energy efficiency and achieving energy conservation and emission reduction [1].

Torque ripple is an inherent issue in BLDCM, with its primary causes being cogging effect, commutation, inactive phase freewheeling, defects in motor design and process, etc [2]. Among these causes, the cogging effect is associated with motor design and has been significantly reduced through optimization of the motor manufacturing process. Inactive phase freewheeling can be mitigated through the use of a special pulse width modulation (PWM). The torque ripple resulting from commutation is attributed to the motor control method, and this torque ripple can reach approximately 50% of the average torque, making commutation the main factor contributing to torque ripple. Therefore, the key to reducing

the overall torque ripple of the motor lies in suppressing the torque ripple caused by commutation.

Currently, the research on suppressing torque ripple primarily focuses on circuit topology, driving methods, and control theory. These approaches include overlapping commutation, torque closed-loop control, front stage converter adjusting DC bus voltage, and optimizing pulse width modulation. The overlapping commutation method for torque ripple suppression involves generating PWM waves with a specific duty cycle for the turn-off/on phases simultaneously during commutation. This ensures that the current change rates are the same [1], thereby stabilizing the non-commutation current. In torque closed-loop control, the dynamic electromagnetic torque of the motor is calculated in real-time and used as feedback. The instantaneous electromagnetic torque is taken as the control reference. By combining this with an efficient closed-loop control algorithm, the torque ripple is reduced [3]. The front stage converter method involves changing the DC bus voltage using a power supply circuit topology that can rise and fall. This adjustment ensures that the bus voltage is equal to four times the amplitude of the back electromotive force (EMF), thereby achieving torque ripple suppression [4]. Optimizing pulse width modulation mainly adopts the new pulse modulation mode of PWM-ON-PWM. This mode eliminates the inactive phase current during non-commutation freewheeling and reduces torque ripple [5].

When the BLDCM is operating in the electric drive conditions, the aforementioned methods for suppressing torque ripple are applicable. However, under braking condition, the working state changes and the equivalent mathematical model also changes accordingly. Therefore, the aforementioned methods are not fully applicable in this condition. In [6], a new PWM-OFF-PWM modulation method is proposed, which is similar to the PWM-ON-PWM modulation used in the electric drive condition but surpasses the freewheeling of the inactive phase. In [7], the torque ripple of six commonly used braking modulation methods is mathematically derived and compared.

The analysis of commutation torque ripple and the derivation of its mathematical expression are presented. The optimal duty cycle of the driving signal and the applicable speed range under different braking modulation modes are determined based on the derived expression. The study in [8] focuses on the commutation torque ripple from the perspective of commonly used braking PWM technology, which includes braking commutation and electric commutation. A comparison of the ripple reduction performance under different braking PWM technologies is conducted based on the corresponding speed range that can reduce torque ripple. Building on the theoretical analysis, a braking torque control method is proposed to reduce torque during the braking process. To address the torque ripple caused by turn-off time being less than turn-on time in PWM-OFF-PWM mode, an improved overlapping commutation method with dynamically adjustable commutation time is presented in [9]. By modulating the turn-off and turn-on phases, the change rates of phase currents in the commutation section are kept the same, and the non-commutation current in the commutation section remains stable. In [10], direct torque control is applied to the braking of BLDCM, enabling closed-loop control of the motor electromagnetic torque and stabilization of torque ripple.

The conventional overlapping commutation method addresses the issue of torque ripple to a certain extent; however, due to potential control lag in the control strategy, the conventional commutation method still faces challenges in mitigating the control failure area associated with torque ripple.

In this paper, an improved PWM-OFF-PWM modulation method is proposed to mitigate the commutation torque ripple of a BLDCM in the braking state. The main contents of this paper are as follows: 1) an analysis of the problems and reasons associated with the torque ripple suppression method based on PWM-OFF-PWM modulation. 2) The invention of an improved overlapping commutation method to address the control fail area problem of torque ripple suppression. 3) Through mathematical analysis, it is concluded that when the out phase and in phase of the duty cycle meet certain conditions during the commutation phase, the sudden change of non-commutation current can be effectively suppressed. As a result, the torque ripple under PWM-OFF-PWM modulation mode is attenuated, and the operational stability of the motor is enhanced.

The remainder of this paper is structured as follows: 1) the mathematical model of BLDCM and the principle of

braking is introduced in the first section, which lays the foundation for the subsequent torque ripple analysis and suppression. 2) The causes of commutation torque ripple under the conventional PWM-OFF-PWM modulation mode are described in the second section. 3) In the third section, the conventional overlapping commutation torque ripple suppression method is suggested, and the existing problems and reasons are pointed out. On this basis, an improved overlapping commutation method is proposed. 4) In the fourth section, the proposed method is verified by experiments. 5) Finally, the conclusion is drawn in the fifth section.

2 The Mathematical Model of BLDCM and the Principles of Modulation

2.1 The Mathematical Model of BLDCM

The three-phase full-bridge inverter circuit of the BLDCM driver is connected to the terminal of the three-phase stator winding, and its equivalent circuit is displayed in Fig. 1. Where R represents the equivalent resistance of the three-phase stator winding, L represents the equivalent inductance of the stator winding, e_a, e_b, e_c are the three-phase back EMF, u_a, u_b, u_c are the three-phase phase voltage, u_n is the reference neutral point voltage, and U_d is the power supply voltage [11].

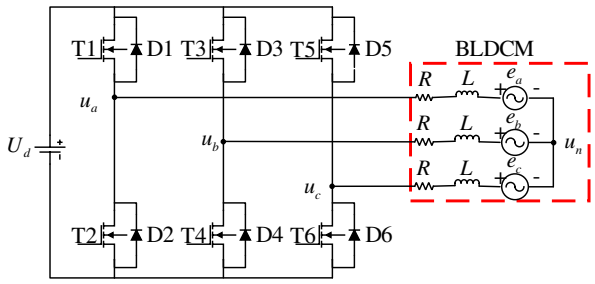

Fig.1 Equivalent circuit of BLDCM

From the above equivalent circuit, the three-phase voltage equation is established:

$$\begin{cases} u_a = Ri_a + L\dfrac{di_a}{dt} + e_a + u_n \\ u_b = Ri_b + L\dfrac{di_b}{dt} + e_b + u_n \\ u_c = Ri_c + L\dfrac{di_c}{dt} + e_c + u_n \end{cases} \tag{1}$$

where i_a, i_b and i_c represent three-phase currents.

The electromagnetic power of BLDCM is the sum of the product of three-phase winding back EMF and three-phase current, which can be expressed as:

$$P_e = T_e\omega_m = e_a i_a + e_b i_b + e_c i_c \tag{1}$$

where T_e is the electromagnetic torque of the motor and ω_m is the angular speed of rotor.

If the magnetic saturation effect and armature reaction are ignored, the back EMF can be described as:

$$E = k_e n \tag{3}$$

where k_e is the back EMF constant and n is the rotor speed. The BLDCM rotates under the joint action of load torque and electromagnetic torque, and its motion equation is:

$$T_e - T_L = J\frac{d\omega_m}{dt} + B\omega_m \tag{2}$$

where J is the rotor moment of inertia and B is the damping coefficient.

2.2 PWM-OFF-PWM Braking Modulation

The trapezoidal back EMF generated when the BLDCM rotates is a periodic signal, and there is a constant value area of 120° electrical angle in both positive and negative half cycles, as in Fig. 2. By applying a constant current within this constant value region of the back EMF, as shown in (2), the motor is able to generate a constant output power. When the polarities of the back EMF and current are opposite, the output torque is in the opposite direction of rotation, resulting in the motor being in a braking state [12]..

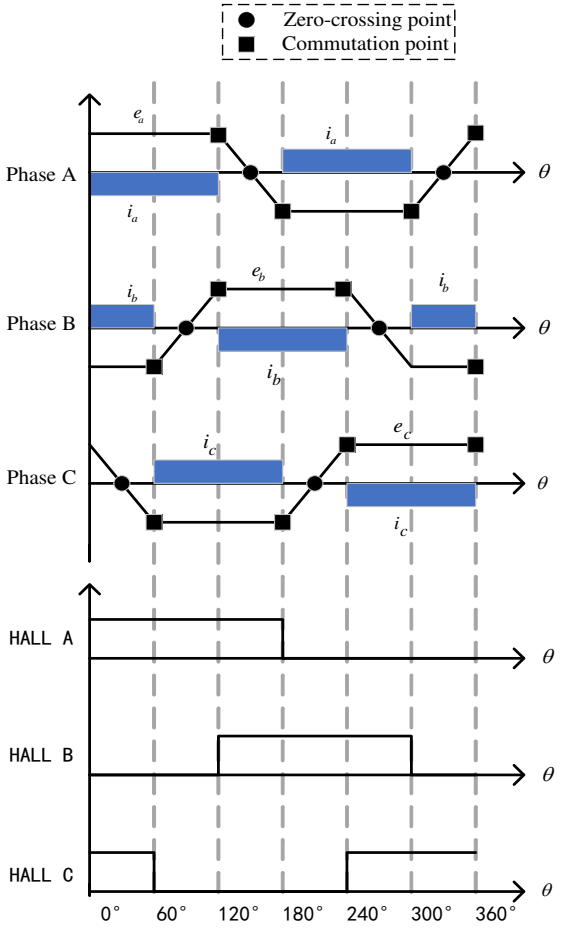

Fig.2 Relationship of position Hall sensor, back EMF and phase current

The PWM modulation of BLDCM includes half- and full-bridge modulations. In half-bridge modulation, only one power transistor is modulated using PWM at a time. On the other hand, in full-bridge modulation, both power transistors of the upper and lower bridge arms are modulated simultaneously.

Only one power transistor is controlled in half-bridge modulation; that is, only one phase can be controlled. Its advantage is that the control method is relatively simple. However, the braking efficiency may be lower than that of full-bridge modulation. In full-bridge modulation, two phases are controlled simultaneously, allowing for the maintenance of dynamic balance in the motor even during braking. By switching the power transistors of the upper and lower bridge arms and adjusting the duty cycle and frequency of the PWM signal, the braking force and efficiency can be more finely controlled to achieve more efficient braking. Compared with half-bridge modulation, full-bridge modulation offers higher control accuracy and braking efficiency, but it also requires more switching devices and control circuits,

thus the cost is higher. Yet, the half-bridge modulation does not output energy during braking and has small switching loss. Therefore, this method has been extensively studied and applied [7].

The half-bridge modulation mode consists of PWM_OFF, OFF_PWM, H_PWM-L_OFF, H_OFF-L_PWM and PWM-OFF-PWM, while the full-bridge modulation mode mainly refers to H_PWM-L_PWM. Among the various modulation modes in the half-bridge modulation mode, PWM-OFF-PWM allows for the elimination of the inactive phase current, unlike the other modes where it still exists. To reduce the torque ripple caused by inactive phase current, PWM-OFF-PWM is selected as the pulse modulation mode in this paper; its braking modulation mode is illustrated in Fig. 3.

When the motor rotates in the forward direction, it passes through six electrical angle areas: I → II → III → IV → V → VI. Conversely, when it rotates in the reverse direction, the sequence changes to VI → V → IV → III → II → I. Consequently, the opening sequence of power transistors T1-T6 when the motor rotates in the forward direction is the opposite of that when the motor rotates in the reverse direction [13].

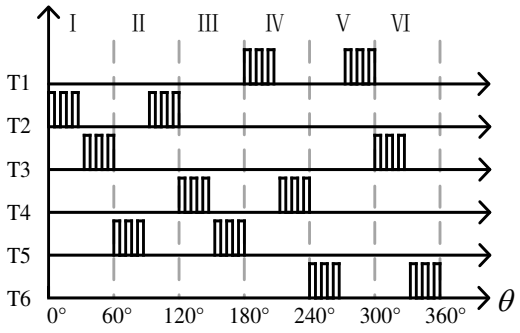

Fig.3 PWM-OFF-PWM modulation

It can be observed from Fig. 2 that the rotor of the BLDCM undergoes commutation once every 60° of electrical angle. In accordance with the six-step commutation method, an electrical angle cycle can be divided into six intervals. The division of intervals can be achieved by encoding the three-phase Hall signals. The relationship between electrical angle and Hall signal encoding is designed in Table 1.

Table 1 Relationship of Hall signal encoding, Hall values, and electrical angle intervals

Hall signal encoding			Hall value	Electrical angle intervals
A	B	C		
1	0	1	5	0° ~60°
1	0	0	4	60° ~120°
1	1	0	6	120° ~180°
0	1	0	2	180° ~240°
0	1	1	3	240° ~300°
0	0	1	1	300° ~360°

3 Analysis of Torque Pulsation in PWM-OFF-PWM Braking Modulation

3.1 Causes of Commutation Torque Ripple

Since the motor winding is an inductive load, the current cannot change suddenly. The current of the turn-off phase will not suddenly change to 0, and the current of the turn-on phase will not abruptly change to that of the turn-off phase before commutation. If the change rate of the on/off phase current is inconsistent, it will result in commutation torque

ripple.

To illustrate this, let's consider the commutation from BA to CA. In this example, phase A is the non-commutating phase, phase B is the turn-off phase, and phase C is the turn-on phase. During this time, there may be three different situations of current change in the commutation section. These variations are depicted in Fig. 4 [14].

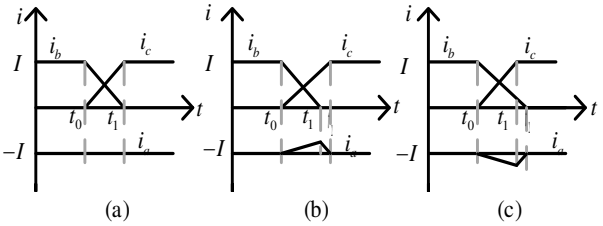

Fig.4 Current variation during commutation

(1) The change rates of the turn-on phase current i_b and turn-off phase current i_c are equal, and the non-commutating current i_a remains constant, as shown in Fig. 4 (a). At this time, the electromagnetic torque of the motor remains constant without commutation torque ripple.

(2) The change rate of the turn-on phase current i_b is greater than that of the turn-off phase current i_c. At time t_1, the turn-off phase current i_b has dropped to 0, while the turn-on phase current i_c has not yet reached the current I before commutation, and the non-commutating current i_a starts to decrease at time t_0, as depicted in Fig. 4 (b). The electromagnetic torque of the motor decreases until the turn-on phase current i_c reaches the current I before commutation; that is, at moment t_2, the non-commutation current i_a remains constant. During the commutation process, current fluctuation and torque ripple are generated [15].

(3) The change rate of the turn-on phase current i_b is less than that of the turn-off phase current i_c. At time t_1, the turn-on phase current i_c has reached the current I before commutation, while the turn-off phase current i_b has not yet decreased to 0, and the non-commutation current i_a begins to increase at time t_0, as in Fig. 4 (c). The electromagnetic torque of the motor increases until the turn-off phase current i_b decreases to 0, that is, at t_2, the current of non-commutating i_a remains constant. During this process, both current ripple and torque ripple also exist.

Therefore, to suppress commutation torque ripple in the process of braking, it is necessary to ensure that the change rates of the turn-off phase and turn-on phase currents are equal in the commutation interval, thus maintaining the stability of the total current in the circuit.

3.2 The Commutation Torque Ripple of PWM-OFF-PWM Modulation

Taking the time of a 60° commutation as an example, at that moment, phase A is in the non-commutation phase, phase B is in the turn-off phase, and phase C is in the turn-on phase. In this commutation section, the upper bridge arm power transistor T5 of phase C is PWM modulated, and the upper bridge arm power transistor T3 of phase B is turned off [7].

When the upper bridge arm power transistor T3 of phase B is off, since the current of the turn-off phase will not directly drop to 0, the diode D4 of the lower bridge arm is turned on, and there is freewheeling in phase B. At this moment, D4, phase B winding, phase A winding, D1 and the battery form a boost circuit, and phase A current flows to the positive end of the battery through D1. When the upper bridge arm power transistor T5 of phase C is on, the upper bridge arm diode D1 of phase A is on, and the phase A current flows to phase C winding through D1 and T5. The current flow is illustrated in Fig. 5.

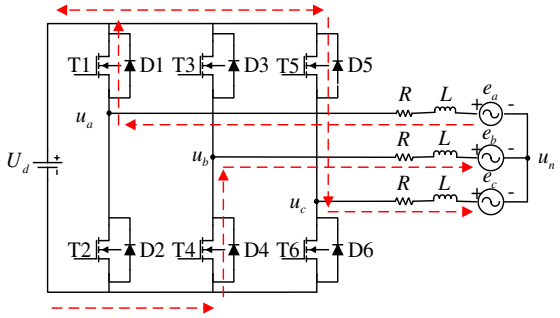

Fig.5 Current flow direction when T5 is On

When the upper bridge arm power transistor T5 of phase C is off, the current in the circuit will not change abruptly due to the motor being an inductive load. The lower bridge arm diode D6 of phase C is on, and there is freewheeling in phase C. The current direction is in Fig. 6.

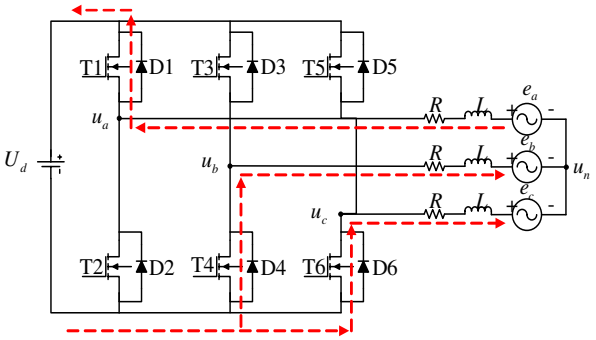

Fig.6 Current flow direction when T5 is Off

Combing (1), the voltage equation of BLDCM is:

$$\begin{cases} u_a = U_{\mathrm{d}} = Ri_a + L\dfrac{di_a}{dt} + e_a + u_n \\ u_b = 0 = Ri_b + L\dfrac{di_b}{dt} + e_b + u_n \\ u_c = D_{on}U_d = Ri_c + L\dfrac{di_c}{dt} + e_c + u_n \end{cases} \tag{3}$$

where D_{on} is the pulse modulation duty cycle of the on-phase.

In the commutation interval, $e_a = E$, $e_b = -E$, $e_c = -E$, combined with (5), the relationship between the current change rate and time is:

$$\begin{cases} \dfrac{di_a}{dt} = \dfrac{(2-D_{on})U_d - 4E}{3L} - Ri_a \\ \dfrac{di_b}{dt} = \dfrac{2E-(1+D_{on})U_d}{3L} - Ri_b \\ \dfrac{di_c}{dt} = \dfrac{(2D_{on}-1)U_d - 2E}{3L} - Ri_c \end{cases} \tag{4}$$

Initial current $-i_a = i_b = I$, $i_c = 0$. Ignoring the stator resistance, the relationship between current and time is:

$$\begin{cases} i_a = -I + \dfrac{(2-D_{on})U_d - 4E}{3L_S}t \\ i_b = I + \dfrac{2E-(1+D_{on})U_d}{3L_S}t \\ i_c = \dfrac{(2D_{on}-1)U_d + 2E}{3L_S}t \end{cases} \tag{5}$$

The electromagnetic torque in the commutation section of braking is:

$$T_e = -\frac{2IE}{\omega_{\mathrm{m}}} + \frac{2(2-D_{on})U_d E - 8E^2}{3L\omega_m}t \tag{6}$$

The torque ripple in the commutation section of braking is [9]:

$$\Delta T_e = \frac{2(2-D_{on})U_d E - 8E^2}{3L\omega_m}t \tag{7}$$

4 The Torque Ripple Suppression of PWM-OFF-PWM Modulation Commutation

4.1 The Ripple Suppression of Commutation Torque and Analysis of Its Applicable Speed Range

The control objective for suppressing commutation torque ripple is to ensure that the torque ripple is equal to zero during commutation, i.e., $\Delta T_e = 0$. By setting (9) of PWM-OFF-PWM commutation torque ripple to zero, the following equation is derived:

$$\Delta T_e = \frac{2(2-D_{on})U_d E - 8E^2}{3L_s\omega_m}t = 0 \tag{8}$$

As can be seen from (10), when $2(2-D_{on})U_d E - 8E^2 = 0$, (10) holds. The open phase duty ratio is:

$$D_{on} = 2 - \frac{4E}{U_d} \tag{9}$$

The duty cycle D_{on} ranges from 0 to 1, (12) can be obtained:

$$0 \le 2 - \frac{4E}{U_d} \le 1 \tag{10}$$

According to the amplitude of back EMF in (3), (12) can be rewritten as [7]:

$$0 \le 2 - \frac{4k_e n}{U_d} \le 1 \tag{11}$$

It can be concluded that the range of motor speed n is $U_d/(4k_e) \le n \le U_d/(2k_e)$, within this range, the commutation torque ripple can be suppressed directly by changing the duty ratio D_{on} of the turn-on phase, while outside the range, this method cannot be practiced. Therefore, the on and off phases are modulated simultaneously using the overlapping commutation method. By ensuring that the change rate of the on and off phases is the same, the speed range in which torque ripple can be suppressed is expanded.

4.2 The Duty Cycle of Overlapping Commutation

With (1), the voltage equation of overlapping commutation is as follows:

$$\begin{cases} u_a = U_d = Ri_a + L\dfrac{di_a}{dt} + e_a + u_n \\ u_b = D_{off}U_d = Ri_b + L\dfrac{di_b}{dt} + e_b + u_n \\ u_c = D_{on}U_d = Ri_c + L\dfrac{di_c}{dt} + e_c + u_n \end{cases} \tag{12}$$

where D_{on} and D_{off} denote the duty cycle of pulse modulation for the turn-on phase and turn-off phase, respectively.

In the commutation interval, $e_A = E, e_B = -E$, $e_C = -E$, combined with (14), the relationship between the current change rate and time is:

$$\begin{cases} \dfrac{di_a}{dt} = \dfrac{(2 - D_{on} - D_{off})U_d - 4E}{3L} - Ri_a \\ \dfrac{di_b}{dt} = \dfrac{(2D_{off} - 1 - D_{on})U_d + 2E}{3L} - Ri_b \\ \dfrac{di_c}{dt} = \dfrac{(2D_{on} - 1 - D_{off})U_d + 2E}{3L} - Ri_c \end{cases} \tag{13}$$

Phase A is non-commutation phase, and if the current of phase A is kept at a constant value, the commutation torque ripple can be suppressed. Ignoring phase resistance, (16) is obtained:

$$\begin{cases} i_a = -I + \dfrac{(2 - D_{on} - D_{off})U_d - 4E}{3L}t \\ i_b = I + \dfrac{(2D_{off} - 1 - D_{on})U_d + 2E}{3L}t \\ i_c = \dfrac{(2D_{on} - 1 - D_{off})U_d + 2E}{3L}t \end{cases} \tag{14}$$

In order to keep the non-commutation current unchanged for $-I$, $(2 - D_{on} - D_{off})U_d - 4E = 0$ should be made. Therefore, when the duty cycle of the turn-on phase and turn-off phase satisfy the following (17), it can be realized [9].

$$D_{on} + D_{off} = 2 - \frac{4E}{U_d} \tag{15}$$

In the running process of BLDCM, the condition $2E < U_d$, namely $n \le U_d / (2k_e)$, and $0 \le D_{on} \le 1$, $0 \le D_{off} \le 1$ are satisfied. In the motor control system, closed-loop controllers such as PID controller and sliding mode controller are generally used to realize the final PWM duty cycle output, and the duty cycle is D_{on}. Combined with (17), D_{off} must meet the following equation:

$$0 \le D_{off} = 2 - \frac{4E}{U_d} - D_{on} \le 1 \tag{16}$$

According to the above analysis, in the engineering implementation process of the conventional overlapping commutation, there is strong coupling between the values of D_{on} and D_{off}. Due to the hysteresis phenomenon in the calculation process of the back EMF and the implementation of the motor control strategy, the duty cycle may not satisfy (17), particularly under sensorless vector control methods, leading to a control failure area and an inability to suppress commutation torque ripple. For example, when the motor speed is high, $4E/U_d$ will be larger. If D_{on} is also large at this time, it may lead to $D_{on} + 4E/U_d > 2$. By calculating (17), D_{off} is less than 0, which does not satisfy $0 \le D_{off} \le 1$, and it is not possible to suppress torque ripple through (17). Similarly, when the motor speed is slow, $4E/U_d$ will be

smaller. If D_{on} is also small at this time, it may lead to $D_{on}+4E/U_d<1$. By calculating (17), D_{off} is greater than 1, which does not satisfy $0\le D_{off}\le 1$, and it is also not possible to suppress torque ripple through equation (17).

4.3 Improved Overlapping Commutation Method

To solve the control fail area problem of the conventional overlapping commutation method in the process of braking, this paper makes further improvements on the overlapping commutation.

The duty cycle D_{on} of the turn-on phase is set to 1, while the duty cycle D_{off} of the turn-off phase is set to 0, combined with current change rate of phase B and phase C in (15) and neglecting the stator resistance, the following results are obtained:

$$\begin{cases} \dfrac{di_b}{dt}=\dfrac{-2U_d+2E}{3L} \\ \dfrac{di_c}{dt}=\dfrac{U_d+2E}{3L} \end{cases} \tag{17}$$

It can be seen from the above (19) that when $\left|-2U_d+2E\right|>\left|U_d+2E\right|$ ($0<n<U_d/4k_e$), there is $\left|di_B/dt\right|>\left|di_C/dt\right|$, that is, the current change rate of turn-off phase is greater than the maximum change rate of the current in the turn-on phase, and the current state is shown in Fig. 4(b); when $\left|-2U_d+2E\right|<\left|U_d+2E\right|$ ($U_d/4k_e<n<U_d/2k_e$), there is $\left|di_B/dt\right|<\left|di_C/dt\right|$, that is, the current change rate of turn-off phase is less than the maximum change rate of the current in the turn-on phase, and the current state is shown in Fig. 4(c). According to the above analysis, the current change rate is different in different motor speed regions. To control the current effectively, the duty cycle of the turn-on phase and turn-off phase can be controlled by dividing the regions.

Combined with (17), the conventional overlapping commutation method is optimized considering reducing the switching times of the power switching devices. The pulse width modulation control method is proposed to only perform the turn-on phase or turn-off phase, as shown in (20), so that the commutation torque ripple can be suppressed in both low and high speed regions of the motor.

$$\begin{cases} D_{on}=2-\dfrac{4E}{U_d},\ D_{off}=0 \quad U_d/4k_e<n\le U_d/2k_e \\ D_{on}=1, \qquad D_{off}=1-\dfrac{4E}{U_d} \qquad 0\le n\le U_d/4k_e \end{cases} \tag{18}$$

In this paper, $4E\le U_d$ ($0<n\le U_d/4k_e$), is defined as the low-speed region; $4E>U_d$ ($U_d/4k_e<n\le U_d/2k_e$) is defined as the high-speed region. According to (20), at low speed, the improved overlapping commutation method has constant conduction of the turn-on phase and pulse modulation is only applied to turn-off phase. At high speed, the turn-off phase has a constant cutoff and only the turn-on phase is pulse-modulated. In this way, through the speed partition method, D_{on} and D_{off} are decoupled to avoid the control fail area.

The action time of the overlapping commutation method is the commutation time. At the 60° commutation point, phase B is the turn-off phase, that is, the target value of phase B current is 0. In (16), phase B current can be expressed as:

$$i_b=0=I+\frac{(2D_{off}-1-D_{on})U_d+2E}{3L}t \tag{19}$$

t in (21) is the time required for the phase B current to drop from the initial value I to 0, which is the commutation time. Therefore, the action time of overlapping commutation can be expressed as [16]:

$$t_{com}=\frac{-3IL}{(2D_{off}-1-D_{on})U_d+2E} \tag{20}$$

The optimal duty cycle of PWM-OFF-PWM modulation in different back EMF ranges is summarized in Table 2.

When the motor control system is in the commutation state, if the pulse modulation mode is PWM-OFF-PWM, the

duty cycle of the turn-on phase and turn-off phase can be obtained according to Table 2, and the overlapping commutation time can be calculated according to (22).

Table 2 Back EMF range and optimal duty cycle for PWM-OFF-PWM modulation

	Range of speed	Range of back EMF	Duty cycle
D_{on}	$\frac{U_d}{4k_e} < n \le \frac{U_d}{2k_e}$	$\frac{U_d}{4} < E \le \frac{U_d}{2}$	$2-\frac{4E}{U_d}$
	$0 < n \le \frac{U_d}{4k_e}$	$0 < E \le \frac{U_d}{4}$	1
D_{off}	$\frac{U_d}{4k_e} < n \le \frac{U_d}{2k_e}$	$\frac{U_d}{4} < E \le \frac{U_d}{2}$	0
	$0 < n \le \frac{U_d}{4k_e}$	$\frac{U_d}{4} < E \le \frac{U_d}{2}$	$1-\frac{4E}{U_d}$

5 Design of control system and analysis of experimental results

5.1 Experiment Platform

The effectiveness and feasibility of the proposed braking control strategy are verified by the experimental platform of two BLDCMs, as in Fig. 7. The left motor serves as the driving motor, responsible for rotating the motor, while the right motor functions as the braking motor, enabling braking. The main parameters of the braking motor are shown in Table 3. In the actual application process, the load connected to the rotor has a moment of inertia. When the motor is braking, it will not stop rotating immediately. This rotational inertia can be simulated by the drag effect of the driving motor.

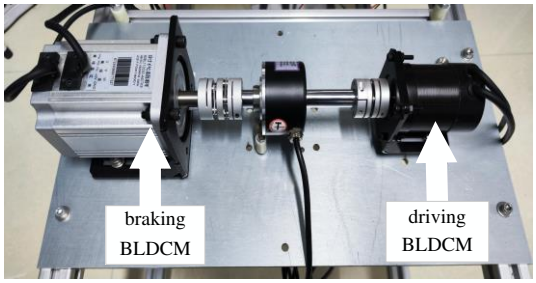

Fig.7 Experimental platform: driving motor and braking Motor

Table 3 Parameters of the braking motor

Parameter	Value
Rated voltage	24V
Phase resistance R	0.21 Ω
Phase inductance L	0.56mH
Number of poles p	2
Back EMF constant k_e	2.36V/kRPM
Inertia of the rotor	0.00119kg • m^2

Combining the definitions of (3) and (20), the cut-off point between high speed and low speed is defined as 2542 RPM, that is, when $0 \le n \le 2542\text{RPM}$, the motor is in a low-speed state, and when $2542\text{RPM} \le n$, the motor is in a high-speed state. The two motors are controlled by two sets of independent control circuits, and the braking motor control system is powered by a 24V lithium battery, as in Fig. 8.

The braking motor control circuit is the main platform for implementing the proposed control strategy, which is composed of three circuit boards. Fig. 9(a) is the main control board, which is equipped with an STM32F103ZET6 core board to facilitate the overall control process. Fig. 9(b) is the drive board, responsible for driving the braking motor. Fig. 9(c) is the current detection board, utilized for detecting three-phase current and bus current.

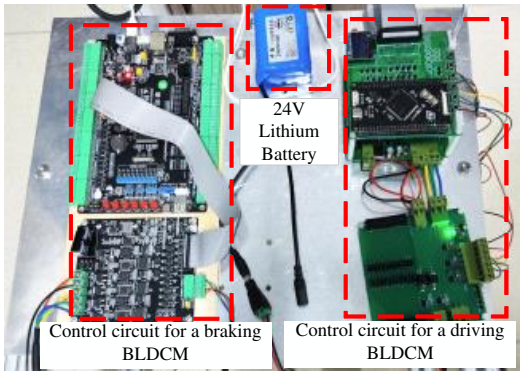

Fig.8 Setting of motor control circuit

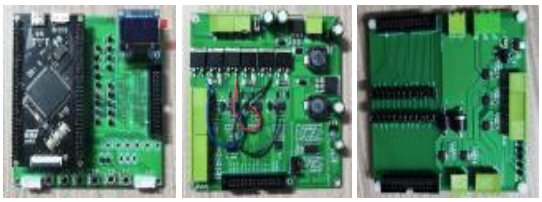

Fig.9 Control circuit of braking motor

5.2 Experiment Result

To verify the proposed commutation torque ripple suppression method, PWM-OFF-PWM modulation with the motor speeds of 1500 RPM and 4600 RPM is tested. Taking the 60° commutation point as an example, the three phases A, B and C are the non-commutation phase, the turn-on phase and turn-off phase respectively.

Fig. 10 shows the phase current waveform of PWM-OFF-PWM modulation mode without torque ripple suppression when the speed is 1500 RPM. The motor speed satisfies $0 < 4k_e n < U_d$ and is in a low-speed state. It is obvious in Fig. 10 that in the commutation interval, the change rates of the off and on phase currents are different, and the non-commutation current has a large fluctuation. Additionally, the commutation torque ripple is directly proportional to the fluctuation in the non-commutation current [**Error! Reference source not found.**]. Consequently, a substantial commutation torque ripple is observed in the commutation region depicted in Fig. 10.

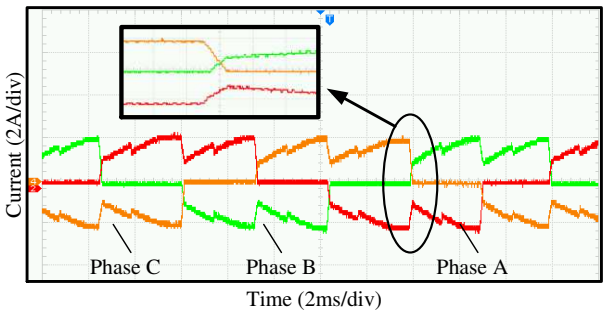

Fig.4 Current waveform of PWM-OFF-PWM without torque ripple suppression (at 1500 RPM)

Fig. 11 shows the phase current waveform under PWM-OFF-PWM modulation after the overlapping commutation torque ripple suppression when the speed is 1500 RPM. Following torque ripple suppression, the rate of change in

current during both the turn-off and turn-on phases is nearly identical during commutation, and the fluctuation of the non-commutation current is significantly improved, effectively achieving torque ripple suppression.

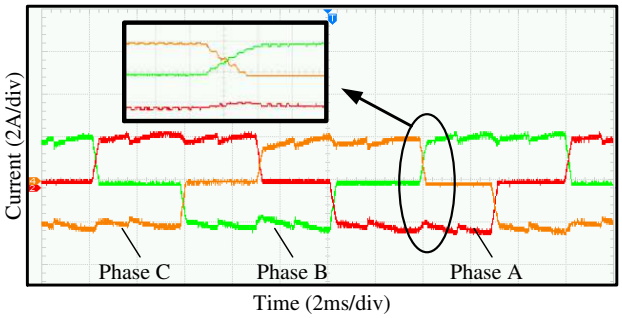

Fig.5 Current waveform of PWM-OFF-PWM with torque ripple suppression (at 1500 RPM)

Fig. 12 is the current waveform under PWM-OFF-PWM modulation without torque ripple suppression when the speed is equal to 4600 RPM. The motor speed satisfies $U_d < 4k_e n \le 2U_d$ and is in high-speed state. The change rates of the off/on phase currents in the commutation region are different, and the non-commutation current exhibits significant fluctuations.

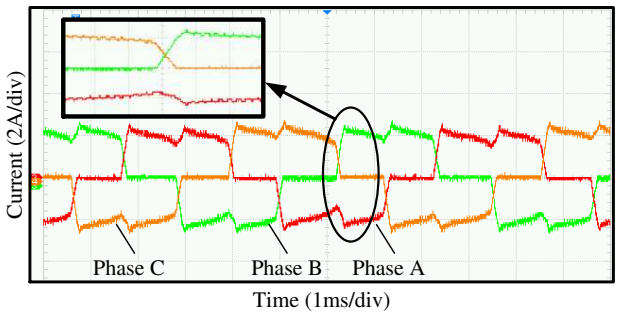

Fig.6 Current waveform of PWM-OFF-PWM without torque ripple suppression (at 4600 RPM)

Fig. 13 is the current waveform after torque ripple suppression by the conventional overlap commutation method when the speed is 4600 RPM. The PWM duty cycle of the main control unit is approximately 42%. It is evident from Fig. 13 that despite the torque ripple suppression, the rates of change in the off/on phase currents are still unequal during commutation, and the non-commutation current fluctuation still exists.

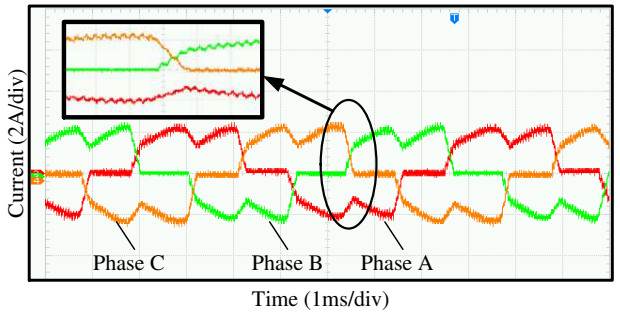

Fig.7 the Current waveform after torque ripple suppression by general overlapping commutation method (at 4600 RPM)

Fig. 14 is the current waveform under PWM-OFF-PWM modulation using the proposed overlapping commutation torque ripple suppression method when the speed is 4600 RPM. After implementing torque ripple suppression, the change rates of the turn-off phase and the turn-on phase currents are almost identical during commutation, and the fluctuation of non-commutation current is significantly reduced.

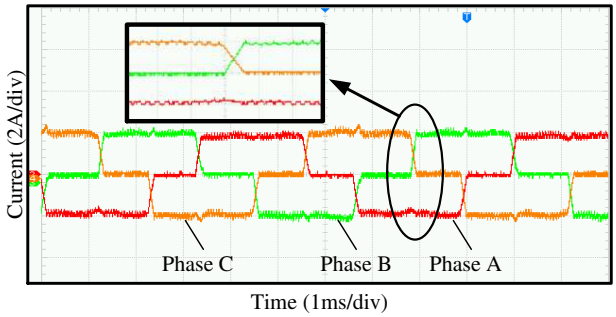

Fig.8 the Current waveform after torque ripple suppression by improved overlapping commutation method (at 4600 RPM)

Comparing the current waveforms under PWM-OFF-PWM modulation mode before and after the commutation torque ripple suppression at high and low speeds, it is proved that the torque ripple suppression method proposed in this paper can suppress the torque ripple in the commutation interval. Upon observing Fig. 13 and 14 at the speed of 4600 RPM, it is illustrated that the proposed overlapping commutation method is more pronounced and significant when the motor speed is high and D_{on} is large.

Fig. 15 shows the turn-on phase and turn-off phase PWM waveforms of overlapping commutation when the speed is 1500 RPM. Pulse modulation is applied to the turn-off phase but the turn-on phase is constantly conducting. If the conventional overlapping commutation method is used, pulse modulation is performed simultaneously for the turn-on and turn-off phases within the commutation interval. In contrast, the overlapping commutation method can reduce the switching times of the power switching devices and extend the service life.

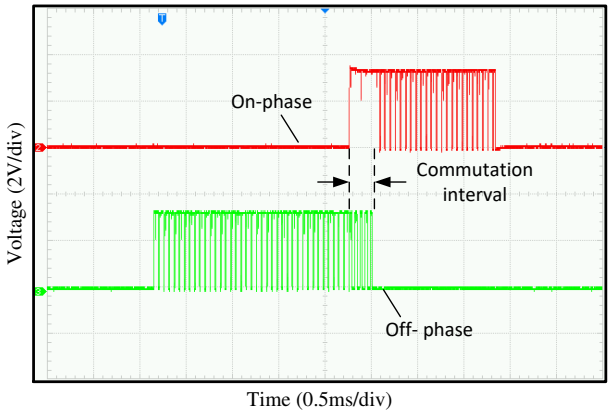

Fig.9 PWM waveforms for on and off phases of overlapping commutation (at 4600 RPM)

Furthermore, this paper presents a statistical analysis of the switching times of the turn-on and turn-off phases within a single commutation interval at different rotational speeds, with the results summarized in Table 4.

Table 4 Switching times of turn-on phase and off-phase during a single commutation at different speeds

Speed (RPM)		Conventional overlapping commutation switch times	Improved overlapping commutation switch times
1000	On phase	13	1
	Off phase	13	7
1500	On phase	10	1
	Off phase	10	5
2000	On phase	9	1
	Off phase	9	4

2500	On phase	8	5
	Off phase	8	1

It is discovered from Table 4 that the switching times of the improved overlapping commutation method in the commutation interval are significantly less than those of the conventional method.

6 Conclusion

Based on the braking condition of BLDCM with PWM-OFF-PWM modulation mode, the main cause of commutation torque ripple is analyzed, and the corresponding mathematical model is established. By analyzing the mathematical model, the time required for commutation and the optimal PWM duty cycle for the on and off phases are determined. Aiming at the problem of commutation torque ripple, an optimized overlapping commutation method is proposed to effectively suppress the torque ripple within a wide speed range. The feasibility and effectiveness of the proposed method are verified by experiments. The main contributions of this paper are as follows:

(1) Based on mathematical derivation, the applicable speed range of commutation torque ripple suppression method for BLDCM in the process of braking is proposed. It is pointed out that in some speed regions, the non-overlapping commutation method cannot achieve commutation torque ripple suppression by only changing the duty cycle D_{on} of the on phase.

(2) The problem of failed control area of commutation torque ripple suppression in braking with the conventional overlapping commutation method is proposed. Due to the strong coupling between D_{on} and D_{off}, as well as the lag phenomenon in the calculation of back EMF and the implementation of motor control strategy, D_{on} and D_{off} may not meet the criteria set in equation (17), resulting in a control fail area and being unable to suppress commutation torque ripple.

(3) An optimized overlapping commutation method is proposed to achieve commutation torque ripple suppression in a wide speed range of the motor. This method only needs pulse modulation of one on/off phase and may effectively reduce the switching times of power switching devices during commutation, which is beneficial for extending the lifespan of the power switching devices and minimizing switching losses.

Data availability

The datasets generated during and/or analyzed during the current study are available from the corresponding author on reasonable request.

Reference

1. Huang, Q., Luo, L., Zhang, Y., & Cao, J. Commutation torque ripple suppression in three phase brushless DC motor using open-end winding. *International Journal of Control, Automation and Systems*, **19(8)**, 2747-2758 (2021).
2. Xia, K., Xu, X., Ding, X., Zhu, L., & Chen, W. Overview of reducing torque ripple for brushless DC motor. *Journal of System Simulation*, **26(7)**, 1417 (2014).
3. Heidari, R., & Ahn, J. W. Torque ripple reduction of BLDC motor with a low-cost fast-response direct DC-link current control.*IEEE Transactions on Industrial Electronics,* **71(1)**, 150-159 (2023).
4. Sun, S., Guo, H., Zhang, Y., Jia, Y., Lv, H., Song, Q., ... & Zhang, Y. Novel modulation method for torque ripple suppression of brushless DC motors based on SIMO DC–DC converter.*Journal of Power Electronics*, **20**, 720-730 (2020).
5. Krishnan, G., Sitbon, M., & Vellayikot, S. Enhanced power factor correction and torque ripple mitigation for DC–

DC converter based BLDC drive. *Electronics*, **12(16)**, 3533 (2023).

6. Bian, C., Duan, P., & XIAO, H. A PWM scheme for regenerative braking of brushless DC motor. *Proceedings of the CSEE*, **39(17)**, 5247-5256 (2019).
7. Han, C. *Research on torque ripple characteristics of breaking modulation methods of BLDCM. unpublished master's thesis*, Xi`an University Of Science And Technology, Xi`an, Shaanxi.https://link.cnki.net/doi/10.27397/d.cnki.gxaku.2020.000303 doi:10.27397/d.cnki.gxaku.2020.000303 (2020).
8. Shi, T., Niu, X., Chen, W., & **a, C. Commutation torque ripple reduction of brushless DC motor in braking operation. *IEEE Transactions on Power Electronics*, **33(2)**, 1463-1475 (2017).
9. Zhou, Q., Shu, J., Cai, Z., Liu, Q., & Du, G. Improved PWM-OFF-PWM to reduce commutation torque ripple of brushless DC motor under braking conditions. *IEEE Access*, *8*, 204020-204030 (2020).
10. Geraee, S., Mohammadbagherpoor, H., Shafiei, M., Valizadeh, M., Montazeri, F., & Feyzi, M. R. Regenerative braking of electric vehicle using a modified direct torque control and adaptive control theory. *Computers & Electrical Engineering*, **69**, 85-97 (2018).
11. Li, Y., Xu, H., & Chen, X. Design and Comparison of Drive Topologies for Stator-Ironless Permanent Magnet Brushless DC Motor. *Transactions of China Electrotechnical Society,* **(24)**, 6619-6631. doi:10.19595/j.cnki.1000-6753.tces.221742 (2023).
12. M U, D. Design and analysis of reconfigurable sensorless brushless DC motor drive for regenerative braking and battery charging in electric vehicle. *International Journal of Circuit Theory and Applications*, **51(11)**, 5283-5304 (2023).
13. Bian, C., Liu, S., **ng, H., & Jia, Y. Research on fault-tolerant operation strategy of rectifier of square wave motor in wind power system. *CES Transactions on Electrical Machines and Systems*, ***5*(1)**, 62-69 (2021).
14. Bai, G., Ma. C. & Lou, K. Torque Ripple Suppression of Brushless DC Motor Based on Improved MPC Strategy. *Modular Machine Tool & Automatic Manufacturing Technique,* **(08)**, 89-93. doi:10.13462/j.cnki.mmtamt.2022.08.021 (2022).
15. Zhou, Q., Shu, J., Cai, Z., Han, C., & Zhang, Y. Optimal duty cycle method to suppress the commutation torque ripple of brushless DC motor in braking mode. *Journal of Electrical Engineering & Technology*, **17(3)**, 1731-1739 (2022).
16. Li, Z., Han, Q., Jia, Y., & Chang, M. Torque Ripple Suppression in Wide Speed Range of Brushless DC Motor Based on Regenerative Boost Inverter. *Transactions of China Electrotechnical Society,* **(06)**, 1725-1736. doi:10.19595/j.cnki.1000-6753.tces.230008 (2024).
17. Yang, M., & Zhou, Y. Ultra-short-term prediction of wind power considering wind farm status. *Resources Environment & Engineering*, 1259 (2019).

Author contributions

C.Z.: Methodology, Review & Editing, Validation, Project administration. S.J.: Writing—Original Draft, Programming. X.L.: Literature & Format Modification, Investigation, Formal analysis. W.Y.: Programming, Review & Editing, Validation.

Competing interests

The authors declare no competing interests